

A Self-Powered Dynamic Displacement Monitoring System Based on Triboelectric Accelerometer

Hua Yu, Xu He, Wenbo Ding, Yongshan Hu, Dongchen Yang, Shan Lu, Changsheng Wu, Haiyang Zou, Ruiyuan Liu, Canhui Lu, and Zhong Lin Wang*

An integrated self-powered dynamic displacement monitoring system by utilizing a novel triboelectric accelerometer for structural health monitoring is proposed and implemented in this study, which can show the dynamic displacement and transmit the alarming signal by accurately sensing the vibration acceleration. The fabricated triboelectric accelerometer based on the noncontact freestanding triboelectric nanogenerator consists of an outer transparent sleeve tube and an inner cylindrical inertial mass that is suspended by a highly stretchable silicone fiber. One pair of copper film electrodes is deposited by physical vapor deposition on nylon film and adhered on the inner wall of the outer tube, while a fluorinated ethylene propylene film with nanowire structures is adhered on the surface of the inner cylindrical inertial mass. The experimental results show that proposed triboelectric accelerometer can accurately sense the vibration acceleration with a high sensitivity of $0.391 \text{ V s}^2 \text{ m}^{-1}$. In particular, the developed accelerometer has superior performance within the low-frequency range. One of the most striking features is that the commercial accelerometer using piezoelectric material is strongly dominated by high-order harmonics, which can cause confusion in computer data analysis. In contrast, the triboelectric accelerometer is only dominated by the base resonance mode.

1. Introduction

With the rapid development of urban construction, more and more infrastructures are being deployed to bring convenience to people's daily life. Consequently, the infrastructure health is of great importance and needs to be monitored all the time. In most cases, the vibration displacement can be used to indicate the infrastructure health status. Traditionally, the displacement measurement is accomplished by using a direct method via the specific equipment, for example, a linear variable differential transducer (LVDT) or a portable laser Doppler vibrometer (LDV). Unfortunately, despite the high accuracy, these direct methods are usually not cost-effective, more time-consuming for field assembly, and sometimes require additional instrument. For example, an indispensable additional reference for LDV is not easy to obtain on the test site.^[1] Conversely, the indirect method estimates the displacement via the measured acceleration, which can achieve moderate accuracy in a more cost-effective way.

The error in the indirect method mainly comes from the sensor drift and unknown initial conditions, and needs to be removed by additional signal processing.^[2] Thanks to the commercialization of the piezoelectric accelerometers, indirect methods have been widely adopted due to easy installation and low cost. However, the complex signal-conditioning electronics, which converts the high-impedance charge signal generated by the sensing element into a usable low-impedance voltage signal, is necessary for piezoelectric accelerometer sensors. Additionally, the output voltage signals of piezoelectric accelerometers are relatively small and vulnerable with the environmental and cable-generated noises, which could lead to erroneous output signals when used in low-frequency environments, and thus a special low-noise cable has to be used for accurate measurements and the system cost will increase significantly.^[3] In this study, a self-powered sensing and monitoring system based on a novel, low cost, easily manufactured triboelectric accelerometer is proposed as an attractive alternative to the traditional displacement measuring system.

The triboelectric nanogenerator (TENG) first invented by Wang and co-workers in 2012^[4] is able to produce electrical output based on triboelectrification and electrostatic induction in response to an external mechanical stimulation.^[5] Its fundamental

Prof. H. Yu, X. He, Dr. W. Ding, C. Wu, H. Zou, R. Liu, Prof. Z. L. Wang
School of Materials Science and Engineering
Georgia Institute of Technology
Atlanta, GA 30332-0245, USA
E-mail: zlwang@gatech.edu

Prof. H. Yu, Y. Hu, D. Yang, S. Lu
Key Laboratory for Optoelectronic Technology and Systems
Ministry of Education of China
Key Laboratory of Fundamental Science of Micro/Nano-Device
and System Technology
Chongqing University
Chongqing 400044, China

X. He, Prof. C. Lu
State Key Laboratory of Polymer Materials Engineering
Polymer Research Institute
Sichuan University
Chengdu 610065, China

Prof. Z. L. Wang
Beijing Institute of Nanoenergy and Nanosystems
Chinese Academy of Sciences
Beijing 100083, China

DOI: 10.1002/aenm.201700565

physics and output characteristics can be attributed to the Maxwell's displacement current.^[6] Specifically, the electric output signals of the TENG directly reflect the impact of the mechanical triggering, so that TENG can be used as an active sensor in responding to external excitation.^[7] The output voltage is a direct measurement of the gap distance, while the output current represents the impact speed. TENG as self-powered active sensor is different from conventional sensors since it can generate an output electric signal itself without an external power supply.^[6] TENG-based sensors have been demonstrated for sensing of motion, pressure, velocity, instantaneous force, and human triggering.^[8–20]

In this study, based on the noncontact freestanding TENG, a novel self-powered accelerometer sensor with the sleeve-tube structure for vibration detection is proposed and fabricated. Moreover, to avoid the infrastructure damage caused by large vibrational displacements, a real-time monitoring system based on the proposed triboelectric accelerometer is developed. It can be used to measure the maximum vibration displacement and regular dynamic responses caused by external random loads such as driving vehicle or strong wind. In particular, the developed triboelectric accelerometer has superior performance within the low-frequency range compared with the commercial piezoelectric accelerometer. One of the most striking features is that the commercial accelerometer using piezoelectric material is strongly dominated by high-order harmonics, which can cause confusion in computer data analysis. In contrast, the triboelectric accelerometer is only dominated by the base resonance mode. Moreover, the proposed self-powered displacement sensing system provides

continuous monitoring with a considerably lower cost, longer lifetime and free maintenance, and all kinds of dynamic response parameters including vibration acceleration, dynamic displacement, and maximum vibration amplitude can be determined and analyzed. The dynamic displacement monitoring system prototype may provide experienced reference on solving problems in the practical application of structural health monitoring.

2. Results and Discussion

With respect to a high-performance TENG applied as an accelerometer, it is crucial to fabricate an effective structure for accurate detection of the parameters generated from bridge vibration. Generally, there is always energy loss in a contact mode TENG due to the inevitable sliding or contact friction between triboelectric layers, resulting in one of the main limitations in monitoring the bridge vibration.^[21] To address this issue, a noncontact working structure was designed by adopting the sleeve-tube as a relative static part while using the inner cylindrical inertial mass as the moving part, which was suspended by a highly stretchable silicone fiber. This noncontact freestanding TENG combines the advantages of effective outputs under low-frequency vibrations triggered by the bridge and a zero energy loss between the triboelectric layers, allowing for the precise health monitoring of the bridge.

Figure 1 shows the device structure and theoretical simulations. As illustrated in Figure 1a, this structure consists of an

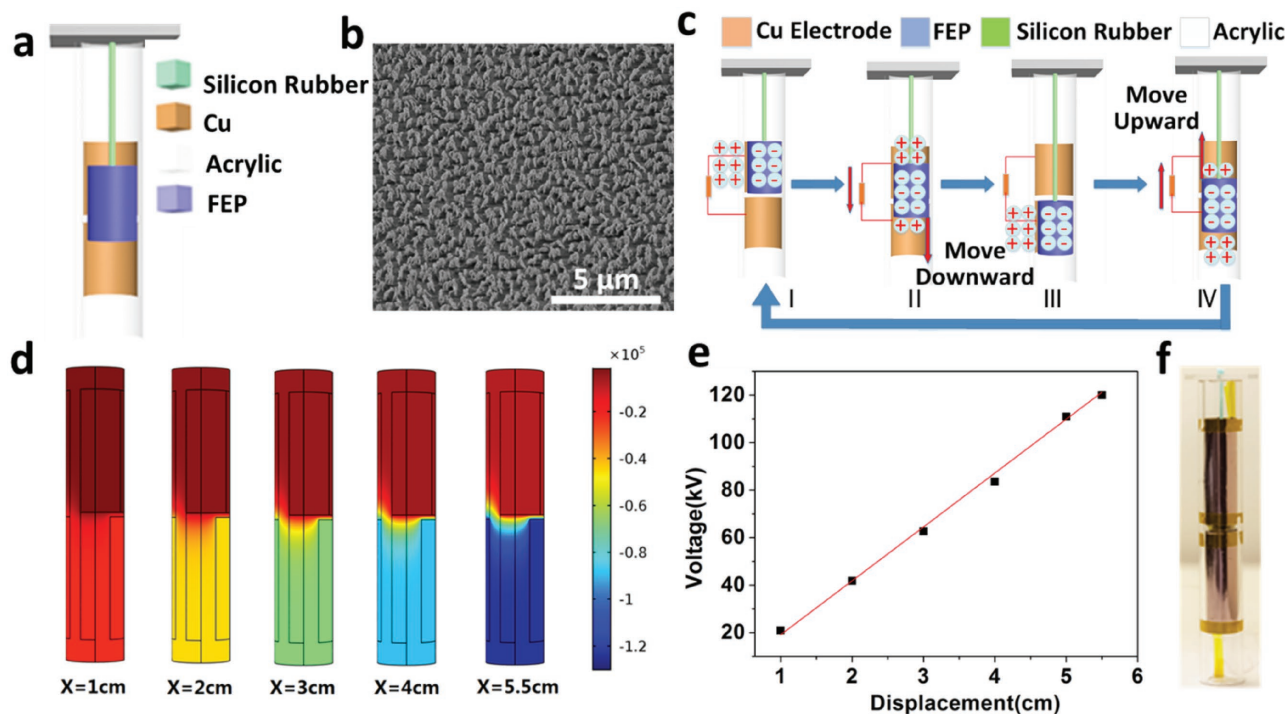


Figure 1. Device structure and theoretical simulations. a) Schematic diagram showing the typical device structure of the proposed triboelectric accelerometer. b) SEM image of the nanowire structures on the FEP film. c) Schematic diagram showing the basic working principle of the triboelectric accelerometer. d) Simulated potential distributions of the triboelectric accelerometer under different displacement of the inner inertial mass. e) The relationship curve between open-circuit voltage of the two electrodes and motion displacement of the inner inertial mass. f) Photograph of the real self-powered triboelectric accelerometer device.

outer transparent sleeve-tube and an inner cylindrical inertial mass suspended by a highly stretchable silicone fiber. The outer tube is made of acrylic and has an inner and outer diameter of 18 and 25 mm, respectively. In our proposed device, two pieces of nylon film (56 mm × 35 mm) are coated with copper (Cu) by physical vapor deposition (PVD) and are pasted on the inner surface of the acrylic tube as fixed triboelectric electrodes. The length of the electrode along the longitudinal vibration direction is 35 mm, and the gap between the two electrodes is 2 mm. The freestanding triboelectric nanogenerator (FTENG) has been demonstrated to be able to operate in noncontact sliding mode. The influence of the gap between the static surface and the moving part surface has been studied theoretically in detail.^[23] Although the triboelectric accelerometer has a good tolerance of a gap distance between the two layers in electricity generation, the performance of the accelerometer sensor such as sensitivity is beginning to decay with the increase of the gap distance between the static surface and the moving part surface. So a relative optimum gap of 2 mm was chosen by regulating the diameters of the outer static sleeve-tube and the inner moving cylindrical inertial mass. The fluorinated ethylene propylene (FEP) film as the freestanding triboelectric layer was adhered on the surface of the cylindrical inertial mass with the diameter of 15 mm and the weight of 32 g. To increase the surface charge density and further enhance the output performance of the TENG, a surface area with high roughness was achieved by fabricating a nanowires array structure on the FEP film through inductively coupled plasma (ICP) reactive-ion etching.^[22] Figure 1b illustrates a scanning electron microscope (SEM) image of the nanowires array on the surface of the FEP film.

As has been proved, when the FEP slides on the surfaces between the two Cu electrodes without contact, the electricity will be generated if the FEP film is already charged due to prior triboelectrification before approaching the electrodes. So the triboelectric charges generated by prior contact can be preserved on insulator surfaces for hours and even days. So the follow-up electricity can be generated by sliding the FEP between the two electrodes even without direct contact, as long as the gap distance between the static surface and the moving part surface is much smaller than the vibrational displacement of the inner FEP film. Thus, the proposed triboelectric accelerometer based on freestanding TENG should be able to operate in noncontact sliding mode.^[23] Owing to the different triboelectric polarity of the FEP and Cu, the electrons will transfer from the Cu electrodes to the FEP film, which renders the FEP film with negative charges and the Cu film electrode with equal amount of positive charges. But it will not generate potential difference between them owing to the electrostatic equilibrium.^[24] For a better illustration of working mechanism, the working principle of the proposed device is shown in Figure 1c. A complete cycle of electricity generation process can be categorized into four phases. First, when the FEP is fully overlapped with the electrode, all the positive charges in the loop will be attracted to the surface of the upper electrode (Figure 1c(I)). Second, when the FEP layer moves toward the lower electrode caused by an external force, the positive charges in the loop will flow from the upper electrode to the lower electrode via the external circuit (Figure 1c(II)). Third, when the FEP moves to the overlapping position of the lower electrode (Figure 1c(III)), all the positive

charges will be driven to the lower electrode. Finally, upward movement of the FEP layer on the mass resonator would generate a reverse current in the load (Figure 1c(IV)), and then be back to the initial position. It should be noted here that the inner cylindrical inertial mass suspended by a highly stretchable silicone fiber will move up and down as a result of the inertia force when subjected to a vertical vibration accelerating force, which causes the proposed device to produce a voltage signal proportional to the force.

The potential distribution at different vibrational displacements of the proposed device can be studied and analyzed using the finite-element analysis software COMSOL. The change of the induced potential difference between the upper electrode and lower electrode at the open-circuit condition under different displacements is shown in Figure 1d. When the inner cylindrical inertial mass is on the top initial position as shown in Figure 1c(I), the potential difference between the upper electrode and the lower electrode is nearly zero. If the inner cylindrical inertial mass starts to move downward from the top initial position because of external vibration, the potential difference between the upper electrode and lower electrode will increase as shown in Figure 1d. When the inner cylindrical inertial mass moves continuously downward displacement from 1 to 5.5 cm, this induced potential difference will be further increased with the increase of moving displacement. At last, the potential difference will reach the maximum when the inner cylindrical inertial mass moves up to the bottom end. On the contrary, in the next half cycle, the upward movement of the inner cylindrical inertial mass will also generate potential difference between the upper electrode and the lower electrode, which will generate potential difference with the opposite polarity across the two electrodes compared with the downward movement. Furthermore, as shown in Figure 1e, a linear relationship between the open circuit voltage of the two electrodes and the displacement of the cylindrical inertial mass has been derived by analyzing the open circuit voltage under a series of different positions of the cylindrical inertial mass. Thus, it is obvious that the open circuit voltage of the proposed device has a very good linearity to the upward and downward motion displacement of the inner cylindrical inertial mass caused by external vibrational acceleration, which provides a theoretical basis for quantitative sensing parameters of vibration acceleration.^[25] Figure 1f displays a photograph of the manufactured self-powered triboelectric accelerometer device. When this device has been installed on external vibrational source, the upward and downward motion of the inner cylindrical inertial mass can result in the electrical output of the device as a result of the relative position change of the tribo charged surfaces between the copper electrode and FEP film. Therefore, it can directly sense the vibration dynamics, including the acceleration and frequency.

The proposed self-powered dynamic displacement monitoring system based on triboelectric accelerometer can be simplified as a second-order single degree-of-freedom spring-mass-damper system with the forced vibration, which consists of a cylindrical inertial mass m , a spring k , and a mechanical damping c . $x(t)$ denotes the displacement of a mass, $y(t)$ is the displacement of the measured object, and $z = x - y$ is the relative displacement between the outer transparent sleeve-tube and the inner cylindrical inertial mass. $f(t) = Fe^{-j\omega t}$ is the harmonic

driven force, where ω is the forcing frequency. The differential equation of the motion with respect to the self-powered triboelectric acceleration sensor system can be modeled as^[26]

$$m \frac{d^2x(t)}{dt^2} + c \frac{dx(t)}{dt} + kx(t) = c \frac{dy(t)}{dt} + ky \quad (1)$$

If the structure is experiencing harmonic vibration, then it can be written as $y(t) = Ye^{j\omega t}$. If let $z(t) = Ze^{j\omega t}$, calculate the velocity and acceleration, and substitute in the above equation, then we have

$$(-m\omega^2 + jc\omega + k)Ze^{j\omega t} = m\omega^2 Ye^{j\omega t} \quad (2)$$

As is well known, $\frac{k}{m} = \omega_n^2$ and $\frac{c}{m} = 2\zeta\omega_n$, where ω_n is the natural angular frequency and ζ is the damping ratio. Substituting them into Equation (2) gives

$$\begin{aligned} \frac{Z}{Y} &= \frac{\omega^2}{(\omega_n^2 - \omega^2) + i(2\zeta\omega_n\omega)} \\ &= \frac{\omega^2}{\omega_n^2 \left(1 - \frac{\omega^2}{\omega_n^2} + i\left(2\zeta \frac{\omega}{\omega_n}\right)\right)} \end{aligned} \quad (3)$$

By denoting $\lambda = \frac{\omega}{\omega_n}$, the magnitude of $\frac{Z}{Y}$ can be written as

$$\left| \frac{Z}{Y} \right| = \frac{1}{\sqrt{\left(\frac{1}{\lambda^2} - 1\right)^2 + \left(\frac{2\zeta}{\lambda}\right)^2}} \quad (4)$$

Obviously, if the condition meets: $\lambda \rightarrow \infty$, then the result is: $|Z| \rightarrow |Y|$. The displacement of the sensing device approaches to the displacement of the vibrational object on the condition that the natural frequency of sensing device is lower enough than that of the measured object. However, the frequency of the measured object, such as the bridge, is usually below several Hz, which requires that the sensing device has a much lower enough nature frequency with a huge enough seismic mass and a soft enough spring. In fact, this kind of sensing device with heavy weight and huge bulk is hard to be fabricated. Therefore, it is extremely difficult to directly measure the displacement of infrastructure by using the sensing device with the architecture of spring-mass-damp system. Whereas, through further analysis for Equation (4), the vibration measurement method based on acceleration is another totally different case. Let us replace $\frac{\omega^2}{\omega_n^2}$ with λ^2 and rearrange to obtain

$$|Z| = \frac{1}{\omega_n^2 \sqrt{(1 - \lambda^2)^2 + (2\zeta\lambda)^2}} \omega^2 |Y| \quad (5)$$

In this equation, $\omega^2|Y|$ represents the base structure's acceleration, and when the coefficient λ approaches to zero, $|Z| \rightarrow \frac{Y}{\omega_n^2}$. Obviously, the displacement of the measured object is proportional to the acceleration as long as the natural

frequency of accelerometer sensor is far higher than that of the measured object, which establishes the theoretical basis. The accelerometer sensor is usually designed to a test instrument with high natural frequency.

So we proposed a self-powered triboelectric accelerometer sensor with the novel sleeve-tube structure based on the above theoretical analysis. The dynamic displacement of the bridge infrastructure is transformed to the acceleration, and then the acceleration leads to the motion displacement of the cylindrical inertial mass. Moreover, the open circuit voltage of the device has a very good linearity to the motion displacement of the inertial mass. In short, the dynamic displacement of the infrastructure is characterized by the electrical signal of the proposed device based on some signal process method. As we know, the natural frequency of the proposed triboelectric accelerometer is very crucial as described above. In practice, the natural frequency of the triboelectric accelerometer is determined by choosing the following parameters of the device structure size and material, such as the elastic modulus of silicon rubber thread E , the cross-sectional area of the silicone rubber thread A , the diameter of the silicone rubber thread d , and the length of silicone rubber thread L . The natural frequency of the proposed triboelectric accelerometer is designed to be 434.8Hz. The quantitative relationship of output voltage, vibration frequency, and acceleration is also determined by Equation (6). The detail analysis and calculation is provided in Section S1 (Supporting Information), and the relationship curves are shown in Figure S2 (Supporting Information)

$$V_{oc} = \frac{Q}{LC_0} \frac{1}{\omega^2} a = \frac{1}{(2\pi)^2} \frac{\sigma S}{LC_0} \frac{1}{f^2} a = k \frac{1}{f^2} a \quad (6)$$

where the parameters are as follows: the output voltage of triboelectric accelerometer V_{oc} , the output charge Q , tribo-charge surface density σ , area S , vibration frequency f , constant coefficient k , and acceleration a ($m\ s^{-2}$).

To investigate the performance of the proposed triboelectric accelerometer, a vibration acceleration testing platform is designed and implemented. It consists of an electrodynamic shaker (Sinocera JZK-5, Labworks Inc.), a commercial accelerometer, a sine servo controller (SC-121), a power amplifier (PA-151), an electrometer, a data acquisition card, our proposed triboelectric accelerometer, and developed dynamic displacement monitoring software. **Figure 2** shows the experimental software and hardware system codesign flow. An electrodynamic shaker is used as an external vibration source with controlled frequency and acceleration. The vibration signal is generated from the sine servo controller, amplified via the power amplifier and finally utilized to control the vibration amplitude and frequency of the electrodynamic shaker. In this way, the acceleration and frequency of the resonator's movement can be accurately controlled. The proposed triboelectric accelerometer device is mounted under the bridge model installed on a shaker together with a calibrated commercial piezoelectric accelerometer for testing under sinusoidal vibration acceleration. Accordingly, the proposed triboelectric accelerometer will undergo excitations and generate electrical output signals. Both the electrical output of the proposed device and the calibrated commercial piezoelectric are recorded on the computer by using the electrometer

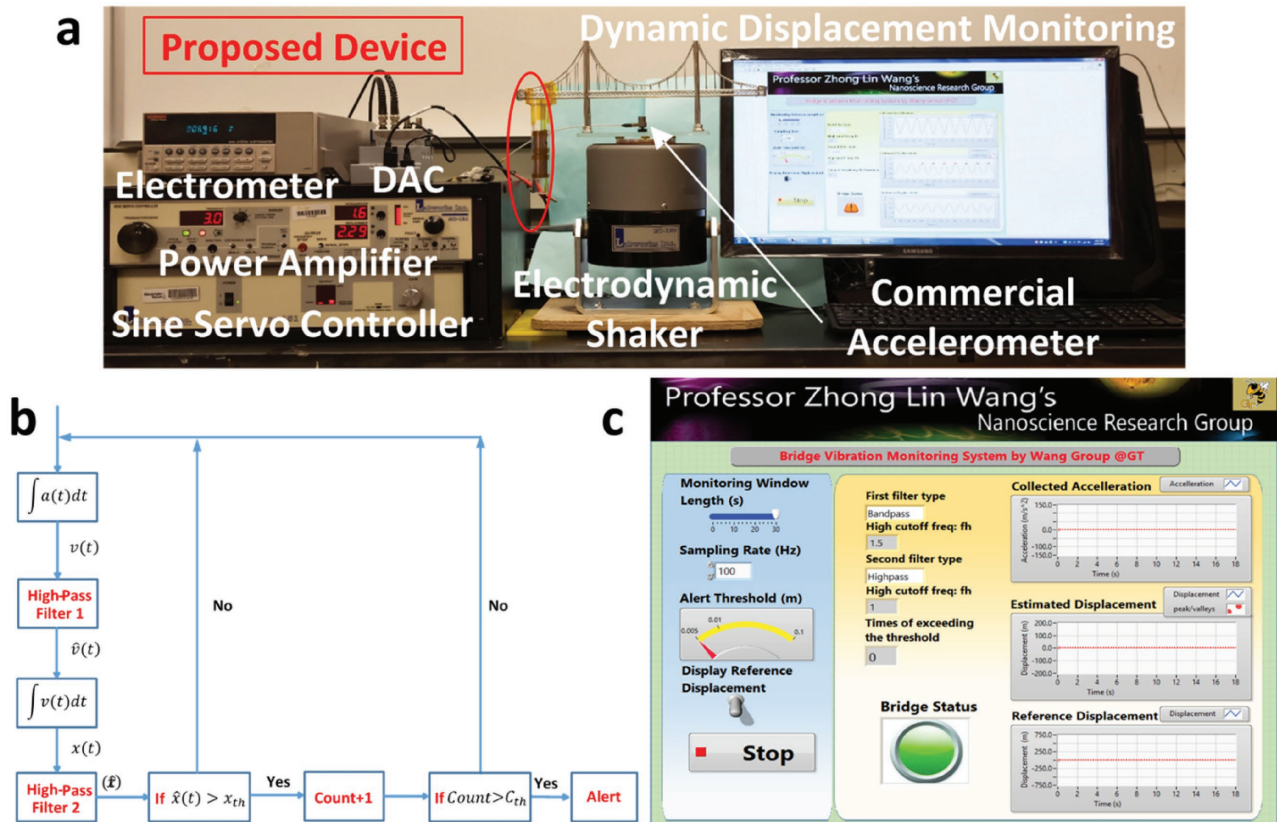


Figure 2. Experimental software and hardware system codesign. a) Photo of the experimental test system. b) Software algorithm flow chart. c) Dynamic displacement monitoring software interface.

and a data acquisition card. The photo of experimental test system is shown in Figure 2a.

The dynamic displacement monitoring system aims to collect dynamic response data of the bridge vibration when it is subjected to random moving vehicle loads, and to help evaluate the safety state of the ridge. Moreover, an alarming signal is autonomously transmitted when the amplitude exceeds the pre-set safety threshold. In this paper, based on the novel proposed triboelectric accelerometer, a modified double integration algorithm is proposed to calculate the displacement from the acquired dynamic acceleration, as shown in Figure 2b. The double integral relationship between the displacement and acceleration is given by Equation (7)

$$\begin{aligned}
 s(t) &= \int_0^t v(\tau) d\tau + s(0) \\
 &= \int_0^t \int_0^t a(\tau) d\tau + v(0)t + s(0)
 \end{aligned}
 \quad (7)$$

where $s(0)$ and $v(0)$ denote the initial displacement and velocity, respectively. It can be observed from this equation that the initial condition ($s(0)$, $v(0)$) has a huge impact on the final displacement estimate. However, in many real world situations, the initial condition is unknown and can cause an accumulative drift error during the double integration. Some advanced algorithm can well compensate the drift error without knowledge

of the initial condition, but are usually in a recursive way and might not be utilized for real-time application. In our application, we aim to estimate the vibration displacement and the initial conditions can be assumed to be zero. In this paper, we modify the filtering-based algorithm to implement the drift error correction. Here, we use the additional high-pass (over 0.1 Hz) filtering after each integral operation. In this way, the baseline distortion of the measured acceleration caused by the external noise and the drift error caused by the integration can be well compensated. Besides, the classical Simpson's 3/8 rule is adopted here to realize the numerical integration with higher accuracy than the standard Simpson's rule, which is given as follows

$$\begin{aligned}
 \int_{t_1}^{t_2} a(\tau) d\tau &\approx \frac{(t_2 - t_1)}{8} \left[a(t_1) + 3a\left(\frac{2t_1 + t_2}{3}\right) \right. \\
 &\quad \left. + 3a\left(\frac{t_1 + 2t_2}{3}\right) + a(t_2) \right]
 \end{aligned}
 \quad (8)$$

To make the system adapt to the real-time monitoring, a point-by-point version of the algorithm is programmed and implemented in LabVIEW 2016. Moreover, if the amplitude of the displacement is continuously exceeding the predefined threshold, the system will give alarm signal to call for maintenance. A real-time dynamic bridge displacement monitoring software system is implemented for demonstration in the

laboratory environment, as shown in Figure 2c. The demonstration video is provided in the Supporting Information. The proposed triboelectric accelerometer is suitable for measuring acceleration along the vertical direction. If it will be applied to measure acceleration along other two directions, the structure of the triboelectric accelerometer should be further improved.

In the following experiments, first, we investigated the relationship between the vibration frequency and the output current of the proposed triboelectric accelerometer. As can be seen from Figure S3 (Supporting Information), the amplitude of short-circuit current increases almost linearly with the increase of vibration frequency. So the vibrational frequency can be measured by the calibration of output short-circuit current for TENG. Second, in order to research on the relationship between the output voltage of the proposed triboelectric accelerometer and vibration acceleration, the electrodynamic shaker was set at different vibration accelerations at a constant frequency, and the output voltage curves are shown in Figure 3. The vibration acceleration of the shaker was set as 13.7, 29.4, 41.2, and 49.0 m s^{-2} , respectively, while the vibration frequency is chosen as 3.0 Hz. Figure 3a–d shows the tested output voltage of the triboelectric accelerometer at several different accelerations, respectively. The overall increasing trend of output voltage is shown in Figure 3e, and all of the output voltage signals are uniform and stable. As is shown in the curve of Figure 3f, the amplitude of output voltage is proportional to the vibration acceleration, which demonstrates an obvious linear relationship by fitting the data with a correlation coefficient of 0.975 and a slope of 3.903. Also, the sensitivity of triboelectric accelerometer could be calculated by the ratio of the numerical value of output voltage and the numerical value of acceleration. So

the sensor has a high sensitivity of $0.391 \text{ V s}^2 \text{ m}^{-1}$, which is beneficial for practical applications. Moreover, similar experiments are also conducted for other low frequencies. The output voltage of proposed triboelectric accelerometer was measured under different vibration acceleration at another constant frequency (2.3 Hz). As shown in Figure S4 (Supporting Information), the correlation coefficient of the linear fitting is 0.994, the slope is 3.916, and the sensitivity of $0.400 \text{ V s}^2 \text{ m}^{-1}$. These test results further verify that the proposed triboelectric device can be as an accelerometer to monitor the vibration by measuring the output voltage.

In order to evaluate the performance of the proposed triboelectric accelerometer, the commercial accelerometer (PCB Piezoelectronics, Inc. ICP SN186880) has been used for quantitative comparison when the vibration frequency is set as 3.0 Hz. Detailed comparison results are shown in Figure 4. Figure 4a provides the comparison of the measured acceleration time history signals between the proposed triboelectric accelerometer and a commercial one, while Figure 4c shows the measured acceleration amplitude spectrum signals (derived from the Fast Fourier transform (FFT)) of time history signals). A partial enlarged view of the time serial acceleration signal is also given in Figure 4b for better illustration. One of the most striking features presented in Figure 4b,c is that the commercial accelerometer using piezoelectric material is strongly dominated by high-order harmonics, which can cause confusion in computer data analysis. In contrast, the triboelectric accelerometer is only dominated by the base resonance mode. This unique advantage is very beneficial for practical applications. In contrast to classical piezoelectric accelerometer, triboelectric accelerometer works best at low frequency ($<5\text{--}10 \text{ Hz}$), which can also be

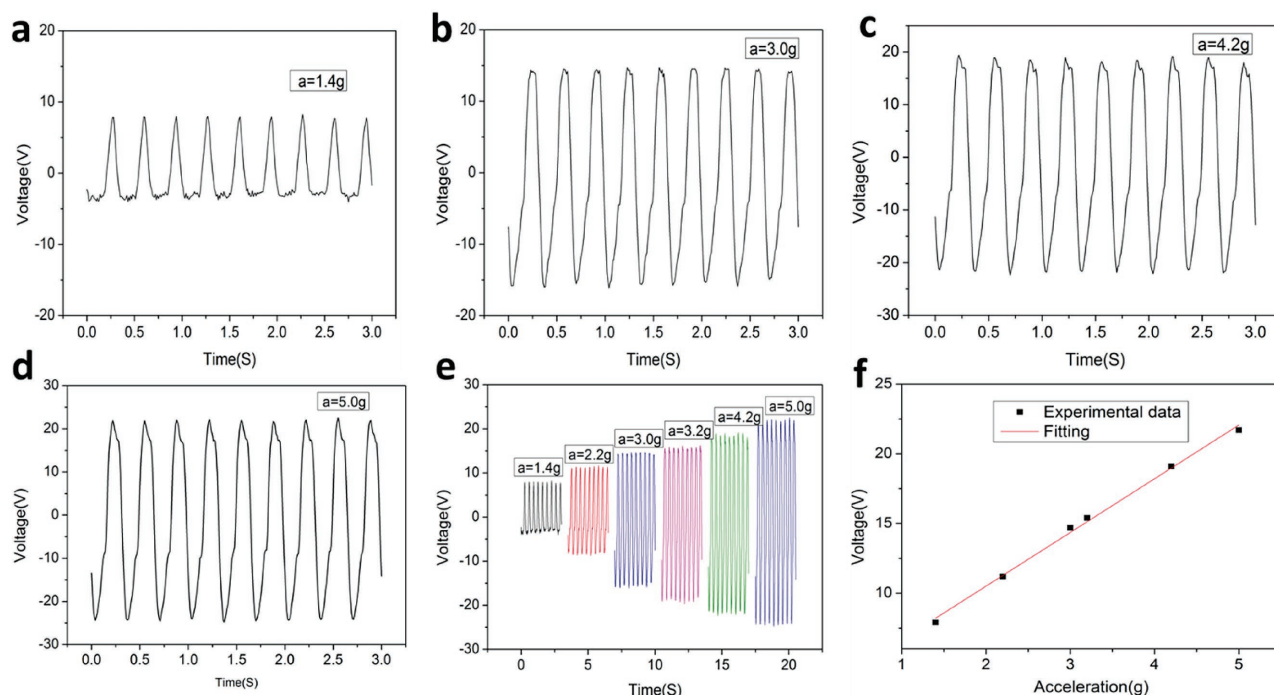


Figure 3. Performances of the triboelectric accelerometer. a–d) Output voltage of triboelectric accelerometer at several specific accelerations. e) Comparison of output voltage of triboelectric accelerometer at several specific accelerations. f) The relationship between the positive peak value of output voltages and the corresponding acceleration.

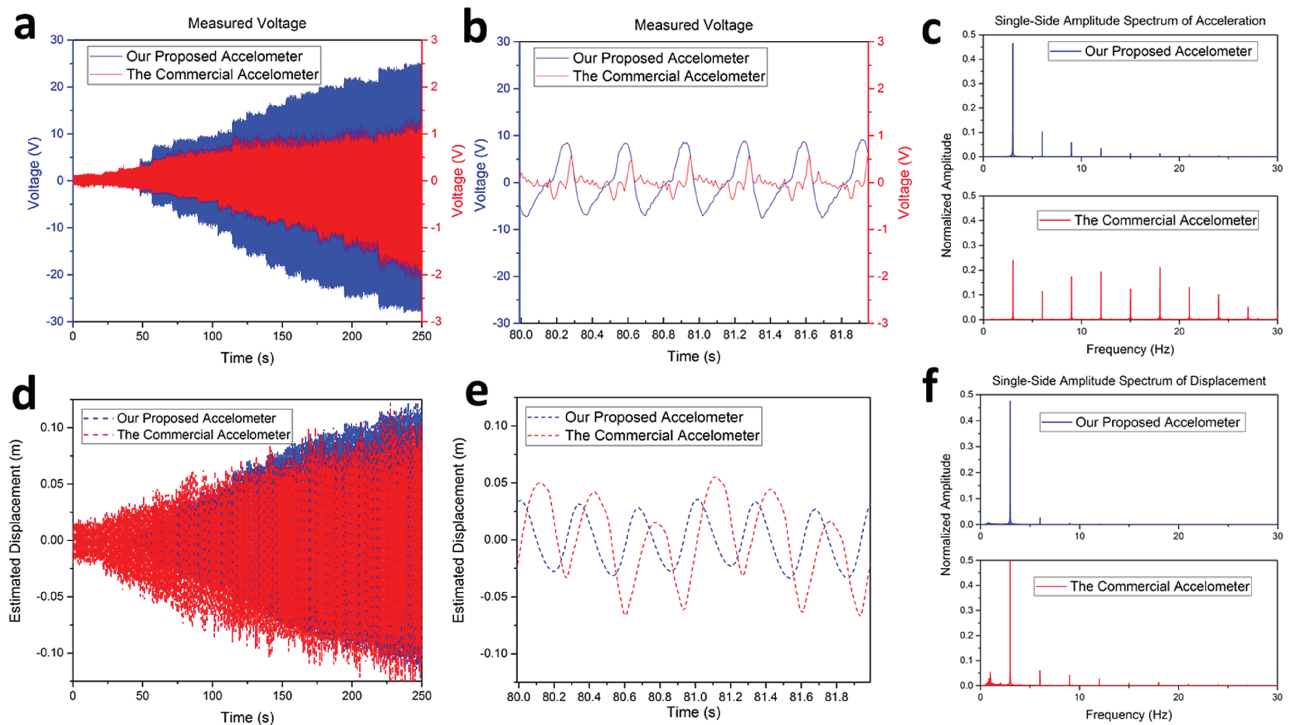


Figure 4. Dynamic displacement monitoring for bridge structural health monitoring. a) Comparison of the measured acceleration time history signal between the proposed triboelectric accelerometer and a commercial accelerometer. b) Partial enlarged view of (a). c) The measured acceleration amplitude spectrum signal of the proposed triboelectric accelerometer and a commercial accelerometer. d) Comparison of the estimated displacement between the proposed triboelectric accelerometer and a commercial accelerometer. e) Partial enlarged view of (d). f) The estimated displacement amplitude spectrum of the proposed triboelectric accelerometer and a commercial accelerometer.

used as a sensor for actively detecting acceleration. The main causes are as follows: First, this is because the frequency has little influence on output voltage and output charge of triboelectric nanogenerator. However, the performance of typical piezoelectric sensor will degrade with the decrease of frequency, especially in low frequency. Second, the output voltage signals of piezoelectric accelerometers are relatively small and vulnerable with the environmental and cable-generated noises, which could lead to erroneous output signals when used in low-frequency environments, and thus a special low-noise cable has to be used for accurate measurements and the system cost will increase significantly. Third, triboelectric accelerometer can be as self-powered active sensor, which is different from conventional sensors since it can generate an output electric signal itself without an external power supply. It can be found that the proposed triboelectric accelerometer is more suitable to apply in low vibration frequency condition than the commercial piezoelectric accelerometer. Moreover, compared with commercial MEMS accelerometer, the proposed triboelectric accelerometer has very low fabrication cost. Of course, the proposed triboelectric accelerometer is only prototype sensor and should be further improved in device structure and fabrication process in order for commercial application. However, triboelectric accelerometer has been shown the splendid prospects and unique merits. The estimated displacement results derived from the measured acceleration are demonstrated in Figure 4d–f. Specifically, Figure 4d shows the comparison of the estimated displacement between the proposed triboelectric

accelerometer and a commercial accelerometer, while Figure 4f shows the estimated displacement amplitude spectrum of the proposed triboelectric accelerometer and a commercial one. A partial enlarged view of the time serial displacement is given in Figure 4e as well. The amplitude spectrum of displacement plots indicates that the low-frequency noise level of our proposed triboelectric accelerometer is very small compared with the commercial accelerometer, which further evaluated the performance of the proposed triboelectric accelerometer especially applied in the low vibration frequency environment. An experimental video demo of dynamic displacement monitoring system based on triboelectric accelerometer for bridge structural health is as shown in Video S5 (Supporting Information).

3. Conclusion

An integrated self-powered dynamic displacement monitoring system based on the novel triboelectric accelerometer sensor is developed. The fabricated triboelectric accelerometer consists of an outer transparent sleeve-tube and an inner cylindrical inertial mass suspended by a highly stretchable silicone fiber. The experimental results show that the generated electric output signals of the fabricated accelerometer are proportional to the vibration acceleration, which can accurately sense the vibration acceleration. Especially, the developed triboelectric accelerometer has more superior performance applying in the lower vibration frequency range (below 5 Hz) compared with

the traditional piezoelectric accelerometer. Moreover, we adopt the accelerometer to monitor the infrastructure health by developing a real-time bridge displacement monitoring system. By timely monitoring of the dynamic displacement of bridge caused by external shock force, the proposed self-powered monitoring system can transmit the alarming signal as soon as the vibrational displacement of bridge exceeds the predefined safety threshold. In a word, the proposed system based on the triboelectric accelerometer will provide a promising and cost-effective solution for the structural health monitoring.

Supporting Information

Supporting Information is available from the Wiley Online Library or from the author.

Acknowledgements

H.Y., X.H., and W.D. contributed equally to this work. Research was supported by the National Natural Science Foundation of China (Grant No. 61074177), Chongqing Research Program of Basic Research and Frontier Technology (Grant Nos. CSTC2014jcyjA40032 and CSTC2015jcyjA40017), the Visiting Scholar Foundation of Key Laboratory for Optoelectronic Technology and Systems, the Hightower Chair foundation, and the “thousands talents” program for pioneer researcher and his innovation team, China, National Natural Science Foundation of China (Grant Nos. 51432005, 5151101243, and 51561145021).

Conflict of Interest

The authors declare no conflict of interest.

Keywords

accelerometer, dynamic displacement monitoring, self-powered sensors, triboelectric nanogenerator

Received: March 1, 2017
Revised: April 5, 2017
Published online:

- [1] B. Xu, G. Song, S. F. Masri, *Struct. Health Monit.* **2012**, *3*, 281.
- [2] J. Zhang, H. Ouyang, J. Yang, *J. Sound Vib.* **2014**, *1*, 1.
- [3] Z. Shen, C. Y. Tan, K. Yao, L. Zhang, Y. F. Chen, *Sens. Actuators, A* **2016**, *241*, 113.
- [4] F. R. Fan, Z. Q. Tian, Z. L. Wang, *Nano Energy* **2012**, *2*, 328.
- [5] C. Zhang, W. Tang, C. Han, F. R. Fan, Z. L. Wang, *Adv. Mater.* **2014**, *22*, 3580.
- [6] Z. L. Wang, *Mater. Today* **2017**, *20*, 74.
- [7] S. Wang, L. Lin, Z. L. Wang, *Nano Energy* **2015**, *11*, 436.
- [8] Y. Yang, H. Zhang, Z. H. Lin, Y. S. Zhou, Q. Jing, Y. Su, J. Yang, J. Chen, C. Hu, Z. L. Wang, *ACS Nano* **2013**, *10*, 9213.
- [9] A. S. M. I. Uddin, G. S. Chung, *RSC Adv.* **2016**, *6*, 63030.
- [10] Q. Shi, H. Wang, T. Wang, C. Lee, *Nano Energy* **2016**, *30*, 450.
- [11] R. K. Gupta, Q. Shi, L. Dhakar, T. Wang, C. H. Heng, C. Lee, *Sci. Rep.* **2017**, *7*, 41396.
- [12] C. Xiang, C. Liu, C. Hao, Z. Wang, L. Che, X. Zhou, *Nano Energy* **2016**, *31*, 469.
- [13] X. Wang, H. Zhang, L. Dong, X. Han, W. Du, J. Zhai, C. Pan, Z. L. Wang, *Adv. Mater.* **2016**, *15*, 2896.
- [14] C. B. Han, C. Zhang, X. H. Li, L. Zhang, T. Zhou, W. Hu, Z. L. Wang, *Nano Energy* **2014**, *9*, 325.
- [15] Y. K. Pang, X. H. Li, M. X. Chen, C. B. Han, C. Zhang, Z. L. Wang, *ACS Appl. Mater. Interfaces* **2015**, *34*, 19076.
- [16] Y. Yang, H. Zhang, Z. H. Lin, Y. Liu, J. Chen, Z. Lin, Y. S. Zhou, C. P. Wong, Z. L. Wang, *Energy Environ. Sci.* **2013**, *6*, 2429.
- [17] L. Dhakar, P. Pitchappa, F. E. H. Tay, C. Lee, *Nano Energy* **2016**, *19*, 532.
- [18] S. W. Chen, X. Cao, N. Wang, L. Ma, H. R. Zhu, M. Willander, Y. Jie, Z. L. Wang, *Adv. Energy Mater.* **2017**, *7*, 1601255.
- [19] K. Y. Lee, H. J. Yoon, T. Jiang, X. Wen, W. Seung, S. W. Kim, Z. L. Wang, *Adv. Energy Mater.* **2016**, *6*, 1502566.
- [20] H. Zhang, Y. Yang, Y. Su, J. Chen, K. Adams, S. Lee, C. Hu, Z. L. Wang, *Adv. Funct. Mater.* **2014**, *10*, 1401.
- [21] Z. L. Wang, J. Chen, L. Lin, *Energy Environ. Sci.* **2015**, *8*, 2250.
- [22] M. H. Yeh, H. Guo, L. Lin, Z. Wen, Z. Li, C. Hu, Z. L. Wang, *Adv. Funct. Mater.* **2016**, *7*, 1054.
- [23] S. Wang, Y. Xie, S. Niu, L. Lin, Z. L. Wang, *Adv. Mater.* **2014**, *18*, 2818.
- [24] Y. Xie, S. Wang, S. Niu, L. Lin, Q. Jing, J. Yang, Z. Wu, Z. L. Wang, *Adv. Mater.* **2014**, *38*, 6599.
- [25] S. Wang, S. Niu, J. Yang, L. Lin, Z. L. Wang, *ACS Nano* **2014**, *8*, 12004.
- [26] T. L. Schmitz, K. S. Smith, *Mechanical Vibrations: Modeling and Measurement*, Springer Science & Business Media, New York, NY 10013, USA, **2011**.